PULSE MODULATION – A NOVEL APPROACH TO GRADIENT-BASED FLOW INJECTION TECHNIQUES

Armando HERBELIN[1,*] and Jaromir RUZICKA[2]

Department of Chemistry, University of Washington, 36 Bagley Hall, Box 351700, Seattle, WA 98195, U.S.A.; e-mail: [1] herbelin@u.washington.edu, [2] ruzicka@chem.washington.edu

Development of a novel system for generation of gradients in flow injection analysis by pulse modulation is described. These user-selectable gradients are created by computer-controlled mixing of two solutions with a total volume as low as 75 µl and can be delivered under incremental or continuous flow conditions. Applications such as automated, single-standard instrument calibration are expected to benefit from high-precision linear gradients (r^2 = 0.99989, n = 55). Gradient methods in biochemisty and immunology such as kinetic measurement of biomolecular interactions will benefit from the small volume of these gradients, especially for analytes with limited availability.

Keywords: Flow injection analysis; FIA; Gradient; Pulse modulation; Analytical methods.

The flow injection (FI) analysis technique[1] has since its inception in 1975 evolved into a widely used analytical tool, described in over 11 000 publications[2,3]. It also has, during past 25 years, evolved from the first generation of continuous FI to discontinuous flow sequential injection (SI) and recently into bead injection (BI) technique[4]. While FI and SI are based on processing of solutions, BI uses a renewable microcolumn of beads for separation and accumulation of target analytes, for manipulation of target microorganisms such as live cells, and for functional assays aimed at drug discovery[5]. Most recently, SI and BI have been downscaled to operate in microlitre range within a microfabricated system[6] ("lab-on-valve").

Each of these methods involves mixing of one or more solutions by dispersion of a bolus of sample in a flow channel under laminar flow conditions. This dispersion naturally forms a gradient that has a form of a tailed Gaussian peak (Fig. 1a). These gradients – and their exquisite repeatability – it is the basis of the performance of all flow injection methods, as their reproducibility secures that all samples and standards will be processed in exactly the same fashion every time. While these natural gradients have been widely exploited in the past for countless FI-based assays, certain ap-

plications would greatly benefit if linear (Fig. 1b), flat/rectangular (Fig. 1c) or even inverse (Fig. 1d) concentration profiles were available. Linear profiles could be used for automated calibration based on a single standard solution. Single-standard calibrations of sensors with slow response times and functional assays or bioligand interaction assays would benefit from availability of flat profiles where the gradient concentration held constant a programmable fraction of the initial solution concentration. Finally, gradient FI titrations could be linearized by using an inverse gradient profile formed from an analyte mixed with the titrant solution.

Methods for generation of gradients for chromatographic applications are widely available. Low-pressure separations in biochemistry commonly use a system of two stirred tanks connected at the bottom to generate linear gradients (straight-wall gradient maker). Commercial gradient controllers for HPLC are widely available from several manufacturers[8]. A pulsed-flow chemistry[9] system has been developed which generates gradients at low pressure for FI applications. Each of these gradient systems typically generates gradients with volumes of 5 to 50 ml and flow rates on the order of 1 ml/min (17 µl/s). These volumes would consume large quantities of
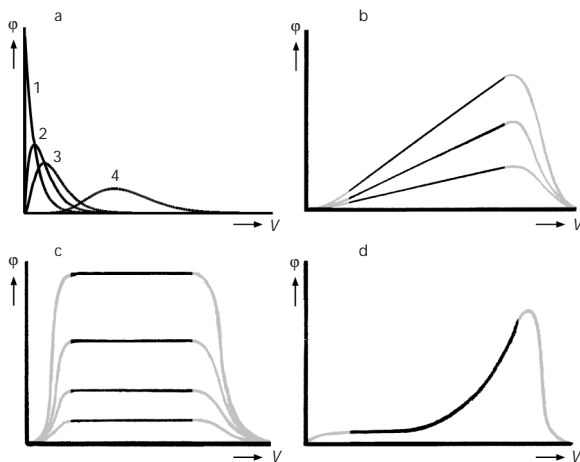

FIG. 1
Gradients in FI analysis plotted as volume fraction of solute #1 (φ) *vs* volume (*v*) in µl. a Theoretical gradient peak shapes according to the mixing tank model[7]: exponential for 1 mixing stage; tailed Gaussian for 2 and 3 mixing stages; and nearly Gaussian for 10 or more mixing stages. b Proposed linear gradients for FI systems. c Proposed "flat" gradients. d Proposed inverse gradient. Grayed areas of the curves in b–d indicate non-ideal portions of the gradients

analyte when applied to FI methods where the gradient is formed from solutions of the analyte. Also, coupling of the gradient FI system to other instruments such as electrospray mass spectrometry requires much lower flow rates, on the order of 1–10 μl/s (ref.[10]) with some electrospray systems operating at 50 nl/min (ref.[11]).

The aim of this work is to develop a method for generating gradients by application of pulse modulation[12] (PM) (Fig. 2a). These gradients should be delivered at flow rates of 1–50 μl/s with a total volume of 75–1 000 μl. The system involves alternate and sequential injection of multiple (20–40) segments of two solutions designated as solute #1 and solute #2. Solute #1 is modeled by injections of a dye. Solute #2 is colorless, identical in these modeling experiments with the carrier solution. The shape of the resulting gradient is monitored by spectrophotometry. The gradient program will be constructed from the theory of pulse modulation. The programmable nature of the method will allow for generation of arbitrary flat, linear, or inverse gradients as shown in Figs 1b–1d.
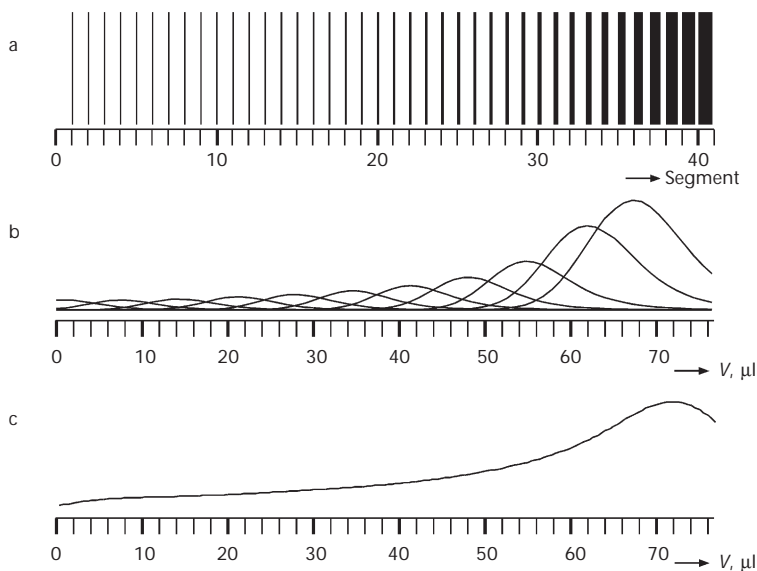

Fig. 2

Schematic of PM gradient method. Desired gradient shape is converted (modulated) into a series of 40 segments (a) with constant volume. Each segment consists of a variable, increasing volume of analyte solution (solute #1) and enough carrier (solute #2) solution to fill the segment volume. When injected in the sequential-injection gradient system, each individual pulse would generate a single SI peak through natural dispersion (b). When all 40 pulses are combined (c), the desired gradient is produced

THEORY

Principles of Pulse Modulation

The pulse-modulation methodology applied to data communications is accomplished in four steps. First, the input signal is modulated to convert the analog signal into digital information. Second, this digital signal is encoded into the square pulses by selecting their width. This digital pulse train is generally encoded at eight times the frequency of the analog signal, a process called oversampling. Third, the signal is transmitted or stored in the digital format. Finally, the signal is demodulated to convert it back into an analog form. Demodulation is accomplished by passing the signal through a low-pass filter which smoothes out the pulses and yields a smooth signal.

To apply pulse modulation to flow injection, a similar four-step process is used. First, the desired gradient shape is entered into a spreadsheet and modulated to determine pulse widths. Next, obtained pulse widths are converted into the volumes of solute #1 and solute #2 to be injected as alternate segments into the low-dispersion gradient coil. Third, the assembled gradient is delivered into the detector at a constant flow rate. Note that demodulation is accomplished by the dispersion process in the flow system, which acts as a low-pass filter.

Practical Limitations of Pulse Modulation

The pulse programs calculated from the pulse modulation method do not generate corresponding fluid gradients for two reasons. First, the FI peak shape is not the same as the output of and electronic low-pass filter – the tailed-Gaussian FI peaks are much wider and thus affect the gradient over a longer range. Second, the practical sampling rate for the FI system is much lower than the ideal rate for electronics, especially for steeply sloped gradients. These problems are overcome by careful characterization of the flow system followed by numerical optimization of the pulse program.

The flow system is characterized by first modeling the behavior of a single peak injected into the gradient coil. The peak shape may be fit to the multiple mixing tank model[7] which can then be used to predict the shape of other injected peaks. Next, the whole PM gradient may be predicted by adding the peak shapes for each pulse in the pulse program (Figs 2b, 2c).

Once the behavior of the flow system is understood, the pulse modulation program is optimized to compensate for the non-ideal gradient shape. Optimization is accomplished by changing the size of individual pulses ei-

ther manually or using an optimization program such as the Microsoft Excel Solver function (Microsoft, www.microsoft.com). Details of this process are given in the discussion section of this paper.

EXPERIMENTAL

Apparatus

The instrumental setup comprised a FIALab 3500 system (FIALab Instruments, www.flowinjection.com) equipped with a six-port selector valve, the liquid handling section of which was replaced by the Lab-On-Valve microfluidic device[6]. The FIALab system has a bidirectional syringe pump furnished with a 250-µl syringe, which was supplemented by a second, external syringe pump (Cavro model XL3000, www.cavro.com) that was controlled by means of a FIALab 3500 accessory port. Software control of the SI system was accomplished with a custom program using Microsoft Visual BASIC 6.0 (Microsoft, www.microsoft.com), the FIALab instruments FIAX COM object to control the SI system, and Ocean Optics OOIWinIP interface software using the DoScan mode. The data acquisition rate was greater than 10 Hz using a PC-compatible computer with 450 MHz processor and 64 MB RAM.

Flow system connections. A schematic of the FIALab/Lab-On-Valve flow system is shown in Fig. 3a. The multiposition valve has been connected to the sample channel situated on the flow-through port (5) and through the central port to the syringe pumps. Peripheral port 2 leads to the dye solution (solute #1) while another peripheral port (3) is connected to solute #2. The holding coil separates the pumps from the valve, while the low-dispersion gradient coil (connected to port 4) is situated downstream from the selector valve leading to the flow-through detector (D). Peripheral ports 1 and 6 are not used in this system.

Spectroscopic measurement. For spectroscopic measurement a PC2000 fiber-optic spectrometer (Ocean Optics, www.oceanoptics.com), furnished with a 600 µm illumination and 225 µm collection fiber-optic cables was employed. A lab-built tungsten lamp was used as a light source. The fiber-optics cables were furnished with 1.588 mm stainless steel tips and mounted in an Upchurch tee fitting (Part # P-722). The tee was modified to accommodate the 1.588 mm tubing and fiber-optic probes. The end of the gradient coil was passed through the tee resulting in a non-dispersive flow cell with an effective optical path length of 0.254 mm, corresponding to a volume of 0.05 µl.

Serpentine coil. The serpentine coil is fabricated by threading tubing through a square grid of holes. Each time the tubing passes through the grid, it is turned 90° to the left or right. The grid of holes was inexpensively prepared by drilling larger holes (1.588 mm) in an electronic circuit board. The openings were smoothed with a 3.175 mm spherical burr to reduce the chance of kinking of the tubing. Care was taken when threading the tubing through the grate because kinks in the coil would give it a very high flow resistance. A photo of the serpentine coil is shown in Fig. 3b. Coils were fabricated using 0.762, 0.508 and 0.254 mm i.d. FEP Teflon tubing. A large gradient coil (≈1 000 µl) was constructed starting with roughly 2.5 m of 0.762 mm i.d. FEP Teflon tubing. Excess tubing was trimmed and the volume of the coil (875 µl) was measured by metering a dye solution through it using the microsyringe. The final volume was reduced from 1 000 to 875 µl which made the coil volume less than the volume of the syringes used in the SI system. Two smaller gradient coils (75 µl) were

constructed using the 0.508 and 0.254 mm tubing (approximately 37 and 148 cm of tubing, respectively). The serpentine coil was connected to the valve port using the shortest practical length of straight tubing (3 cm). Care was taken to insert this tubing all the way through the fitting and into the port, in order to eliminate undefined mixing which could take place within a dead volume.

Reagents

Solutions of a dye, 0.5 mM Bromothymol Blue (Merck) in 0.025 M $NaBO_3$ were used as a tracer to characterize the dispersion of the flow system and to investigate the form of the concentration gradient. This solution is referred to in the text as solute #1. As solute #2, 0.025 M $NaBO_3$ was used. Deionized water was used as a carrier solution to prevent contact between buffer solutions and the syringe pump. All spectrophotometric measurements were carried out at 621 nm, near the absorbance maximum for Bromothymol Blue.
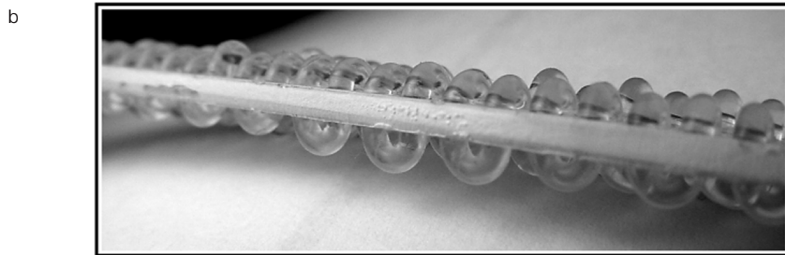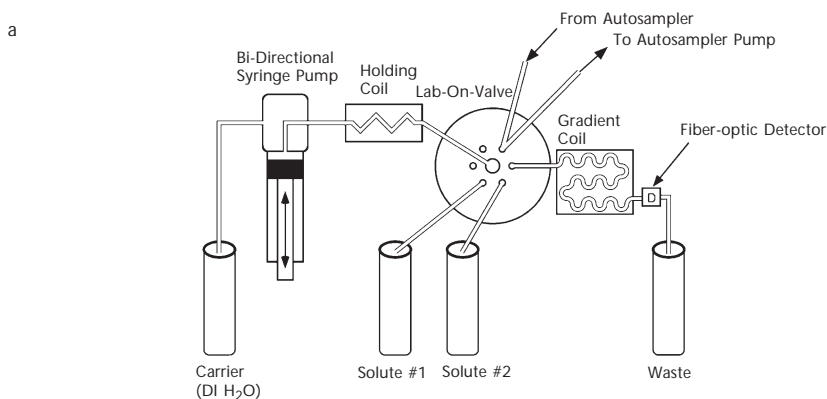
FIG. 3

a Typical SI system (FIALab 3500, FIAlab Instruments, www.flowinjection.com) modified for gradient techniques. The system uses a 250-μl or 1 000-μl syringe and has been upgraded with the Lab-On-Valve microfluidic device[6]. b Photograph of the serpentine gradient coil constructed with 0.254 mm i.d. FEP Teflon tubing

RESULTS AND DISCUSSION

Low-Dispersion Gradient Coil

The intended application of the PM gradients to bead injection requires that the entire gradient is assembled in the holding coil before being delivered by continuous, forward flow into the detector. As the individual segments pass through the gradient coil, they are dispersed and combine to create the final gradient shape. Unfortunately, the dispersion in a tube can be quite high, especially as the gradient volume increases. For this reason, the dispersion in the gradient coil should be minimized.

The dependence of dispersion on the holding coil geometry has been well established (ref.[13], p. 113). Generally, by bending or turning tubing, the laminar flow is disturbed and radial mixing is enhanced which leads to lesser axial zone spreading. Lower dispersion is realized as the turns become tighter and more frequent. Typical geometries include helical, crimped, knotted, knitted, and serpentine coils. The helical coil is fabricated by simply winding the tubing around a cylinder. The holding coil was fabricated in this fashion by winding tubing around a 1-cm-diameter Teflon rod. In the crimped coil, the tubing is sharply bent every 0.5–2 cm causing a sudden change of flow direction. Crimping requires rigid materials such as PEEK or stainless steel. Knotted and knitted coils have much lower dispersion: however, they are difficult to fabricate in a reproducible manner. Serpentine coils have been used in post-column liquid chromatography to reduce dispersion when a length of tubing is needed to carry out derivatization of analytes *prior* to their detection. The closely spaced, tight turns in the serpentine coil effectively disturb the laminar flow and enhance radial mixing.

Selection of Syringes

The pulse-modulation technique involves series of alternate small injections of solute #1 and solute #2 as well as moving of the resulting gradient by means of carrier solution. Typically, for the large 875-μl low-dispersion holding coil, solute injections range from 1.7 to 10 μl and require delivery resolution on the order of 0.1 μl from the syringe pumps. The scaled-down system (75 μl holding coil) requires a resolution on the order of 0.01 μl. The syringe pumps were equipped with 1 000-μl syringes for the large (875 μl) low-dispersion (serpentine) coil or 250-μl syringes for each of the small (75 μl) low-dispersion (serpentine) coils.

With the 1 000-µl syringes, the high-resolution Cavro syringe pumps typically operate with 3 000 steps per stroke, roughly 3 steps per µl. In this mode, the maximum resolution for the syringe pump would be one step or 0.33 µl. For this work, the syringe pumps were programmed to operate in microstepping mode with 24 000 steps per stroke and a resolution of 0.042 µl. In practice, however, the resolution is somewhat lower. Generally the microstepping mode has improved performance over the standard 3 000 steps/stroke mode but not by the full amount. As a rule, expect improvement by a factor of four or five instead of eight or approximately 0.07 µl, which is plenty for the required resolution. With the 250-µl syringes, the resolution is improved by a factor of 4, or approximately 0.02 µl, close to the required performance. While 50- and 100-µl syringes are available for the pumps, the 250-µl syringes were chosen to simplify the general operation of the sequential injection system.

Experimental Protocol for Pulse-Modulation Time Programming

The basic principle for application of pulse modulation to sequential injection is that many small plugs of a solute #1 are injected into the holding coil. The size of solute #1 plugs are varied according to the results of the modulation process as explained in the theoretical section of this paper. Using pulse width modulation, a fixed segment size is used so after the solute #1 plug is injected, the rest of the segment is filled by injecting solute #2. After all of the segments have been injected, the gradient is delivered at continuous flow to the detector. Since approximately 40 segments are used, implementation of this scheme may have resulted in roughly 160 turns of the multiposition valve if the system programming is not optimized. Careful design of the system programming cuts this number to 80, saving both time and instrument wear. The basic steps are as follows:

a) The valve is turned to the solute #2 port and then an excess of this solution is aspirated into the holding coil (Fig. 4a).

b) The valve is turned to the solute #1 port and the first volume segment is aspirated into the same holding coil (Fig. 4b).

c) The valve is turned to the gradient coil port and the entire volume segment, including solutes #1 and #2, is dispensed into the gradient coil (Fig. 4c).

d) Steps b, c are repeated for each of forty segments (Fig. 4d).

e) The syringe pump is refilled and then the entire gradient is delivered to the detector at a constant flow rate (Figs 4d, 4e).

Note that the first segment injected into the gradient coil is the first one to come out, commonly referred to as a first-in-first-out system. This design has the advantage that each segment follows the same flow path and is thus dispersed by the same amount. The only difference between the different segments is that the first segments start and stop many times on their way through the gradient coil and the last segments go through under continuous flow. However, the difference in dispersion due to this effect is small.

Additional approaches were tested, including the addition of a second syringe to the lab-on-valve system. In this design, both syringes were connected to the central port of the lab-on-valve by a separate holding coil. Each holding coil was filled with one of the solutes (#1 or #2) and the gradient would then be delivered by dispensing to the gradient coil from each
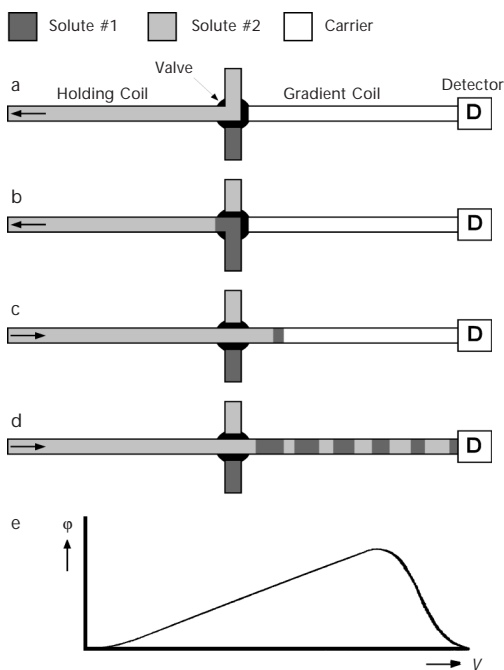

FIG. 4

Steps in the gradient injection method. a An excess of solute #2 is aspirated into the holding coil (Fig. 3a). b A programmed amount of solute #1 is aspirated into the holding coil. c The whole segment volume (solute #1 and solute #2) is dispensed into the gradient coil. d Steps b, c are repeated for each segment in the gradient program. e The gradient is delivered to the detector which records the gradient shape

syringe in turn. Once the gradient was loaded into the gradient coil, one syringe was used to deliver the gradient at a constant flow rate. The two-syringe design reduced the total number of valve turns to three and significantly reduced the time required to build the gradient. Unfortunately, for the small gradients (75 µl), the dispersion from the merging point through the multiposition valve was too large for the desired gradient production. Details of the final gradient protocol are shown in Table I.

Characterization of the Pulse-Modulation Flow System

Design of the pulse-modulation gradient system requires an understanding of how injected plugs of solutes #1 and #2 solution are dispersed through the gradient coil. Important factors include the overall dispersion and peak shape.

Overall Dispersion

In the first experiment, $S_{1/2}$, the segment volume resulting in a peak height, C^{max}, equal to one half of the undiluted concentration, C_0, was determined for the system. $S_{1/2}$ can be measured by injecting an increasing series of single segments of dye into the gradient coil and plotting C^{max} against the injected volume, S_v. $S_{1/2}$ is calculated from this curve by a non-linear fit to the following equation (ref.[13], p. 119).

$$\frac{C^{max}}{C_0} = 1 - e^{-\frac{0.693 S_v}{S_{1/2}}} \tag{1}$$

While this equation was derived for a single mixing stage, the use of $S_{1/2}$ is a generally accepted practice. The values were found to be $S_{1/2} = 200$ µl for the large gradient coil (875 µl, 0.762 mm i.d.), $S_{1/2} = 20$ µl for small coil #1 (75 µl, 0.508 mm i.d.), and $S_{1/2} = 7.5$ µl for small coil #2 (75 µl, 0.254 mm i.d.).

Peak Shape

The empirical model of the gradient system depends on precise prediction of the peak shape for each pulse in the gradient. The numerical function used to define peak shape uses parameters for peak size, position, width, and tailing. Prediction of these parameters will depend on the size of an in-

TABLE I
Sequential-injection steps for PM gradients. Step-by-step procedures are given for loading the 75-µl gradients

Step	Description
1	Turn valve to port 3 and aspirate 250 µl of solute #2 into the holding coil at 10 µl/s
2	Turn valve to port 4 and dispense 50 µl of solute #2 into the gradient coil
3	Enable high-resolution mode of syringe pump (Syringe Command "N1R")
4	Turn valve to port 2 and aspirate programmed volume of solute #1 (see below)
5	Turn valve to port 4 and dispense 1.875 µl into the gradient coil (consists of both solutes #1 and #2)
6	Repeat steps 4 and 5 for each pulse in the modulation program
7	Disable high-resolution mode of syringe pump (Syringe Command "N0R")
8	Fill syringe with carrier solution
9	Start data acquisition and empty syringe through the gradient coil and detector

Desired gradient	Pulse sizes, µl
Flat 0.10	0.387, 0.366, 0.320, 0.251, 0.167, 0.088, 0.044, 0.059, 0.134, 0.225, 0.250, 0.166, 0.076, 0.127, 0.209, 0.170, 0.121, 0.158, 0.176, 0.147, 0.147, 0.165, 0.158, 0.150, 0.154, 0.162, 0.155, 0.153, 0.157, 0.156, 0.155, 0.156, 0.157, 0.154, 0.158, 0.155, 0.153, 0.162, 0.171, 0.171
Flat 0.25	0.922, 0.882, 0.786, 0.636, 0.447, 0.261, 0.141, 0.146, 0.296, 0.511, 0.616, 0.476, 0.240, 0.260, 0.469, 0.488, 0.336, 0.326, 0.434, 0.424, 0.354, 0.375, 0.416, 0.394, 0.372, 0.389, 0.404, 0.386, 0.382, 0.393, 0.398, 0.379, 0.389, 0.402, 0.377, 0.397, 0.387, 0.400, 0.443, 0.443
Flat 0.50	1.815, 1.743, 1.565, 1.279, 0.914, 0.549, 0.300, 0.291, 0.565, 0.987, 1.225, 0.992, 0.519, 0.484, 0.882, 1.004, 0.735, 0.627, 0.816, 0.881, 0.734, 0.724, 0.827, 0.797, 0.743, 0.785, 0.799, 0.765, 0.771, 0.796, 0.778, 0.770, 0.778, 0.785, 0.779, 0.786, 0.757, 0.812, 0.885, 0.886
Flat 1.0	1.875, 1.875, 1.875, 1.875, 1.875, 1.875, 1.875, 1.875, 1.875, 1.441, 1.148, 1.162, 1.405, 1.687, 1.818, 1.734, 1.542, 1.411, 1.435, 1.565, 1.666, 1.645, 1.537, 1.467, 1.506, 1.591, 1.626, 1.588, 1.529, 1.509, 1.547, 1.595, 1.597, 1.550, 1.507, 1.534, 1.651, 1.757, 1.779, 1.778
Linear 0.25	0.036, 0.054, 0.064, 0.080, 0.087, 0.098, 0.101, 0.110, 0.114, 0.127, 0.141, 0.148, 0.161, 0.166, 0.179, 0.185, 0.199, 0.205, 0.216, 0.226, 0.234, 0.247, 0.251, 0.266, 0.272, 0.284, 0.291, 0.302, 0.313, 0.320, 0.332, 0.339, 0.352, 0.356, 0.373, 0.377, 0.386, 0.406, 0.429, 0.443
Linear 0.50	0.000, 0.063, 0.148, 0.206, 0.227, 0.214, 0.189, 0.181, 0.206, 0.255, 0.298, 0.320, 0.316, 0.321, 0.348, 0.379, 0.402, 0.414, 0.425, 0.444, 0.471, 0.496, 0.512, 0.528, 0.539, 0.561, 0.588, 0.612, 0.626, 0.634, 0.651, 0.683, 0.719, 0.740, 0.737, 0.708, 0.713, 0.812, 1.001, 1.237
Linear 0.75	0.113, 0.161, 0.197, 0.234, 0.260, 0.288, 0.311, 0.327, 0.351, 0.376, 0.416, 0.456, 0.477, 0.501, 0.531, 0.560, 0.593, 0.616, 0.648, 0.678, 0.700, 0.737, 0.763, 0.789, 0.822, 0.848, 0.877, 0.907, 0.936, 0.962, 0.991, 1.028, 1.045, 1.077, 1.114, 1.132, 1.162, 1.223, 1.278, 1.314
Inverse	0.195, 0.190, 0.165, 0.128, 0.091, 0.053, 0.041, 0.054, 0.097, 0.148, 0.150, 0.107, 0.073, 0.121, 0.156, 0.124, 0.121, 0.153, 0.157, 0.146, 0.167, 0.181, 0.179, 0.196, 0.211, 0.223, 0.237, 0.259, 0.284, 0.304, 0.338, 0.382, 0.414, 0.493, 0.560, 0.650, 0.853, 0.885, 0.994, 1.300

dividual pulse as well as on the position in the gradient program. The pulse position is important because the first pulse advances through the gradient coil in 39 short steps as the other pulses are injected while later pulses travel through the gradient coil in a few short steps, followed by a constant flow rate when the gradient is delivered to the detector.

To measure the dependence, the instrument was run using gradient programs consisting of single non-zero pulse and 39 pulses with a programmed volume of 0 µl for solute #1. All other experimental conditions were identical to those used for gradients: 75 µl, 0.254 i.d. gradient coil with a 10 µl/s delivery flow rate and a 1.88 µl segment size. The size and position of the single pulse was varied to cover a range of pulse sizes (0.1, 0.2, 0.5, 1.0, 1.88 µl) and positions (1, 5, 10, 20, 40).

The single FI peaks in each of these runs were fit using the tank in series dilution equation described by Levenspiel[7] and applied to FI by Ruzicka (ref.[13], Eq. (3.6.10)):

$$C(t) = C_0^* \left(\frac{t}{\overline{T}} \right)^{N-1} \frac{1}{(N-1)!} e^{-\frac{t}{\overline{T}}}, \tag{2}$$

where $C(t)$ is concentration of component at the output of the system at time t, C_0^* is the initial concentration of the component in the first mixing stage, N is the number of mixing stages, and $\overline{T}$ is the mean residence time. For application of Eq. (2) to this system, some modifications are necessary. The equation is converted to volume scale: time t is replaced by volume v of solvent passed through system and mean residence time $\overline{T}$ is converted to a mean residence volume, $\overline{V}$. To accommodate fractional values of N, the factorial term $(N-1)!$ is replaced by Euler's gamma function $\Gamma(N)$. Volume offset v_0 is introduced to shift the peak position. To summarize this model may be represented as follows:

$$\varphi(v) = \left\{ \begin{array}{ll} 0, & v < v_0 \\ \dfrac{V_i^*}{\overline{V}} \left(\dfrac{v - v_0}{\overline{V}} \right)^{N-1} \dfrac{1}{\Gamma(N)} e^{-\left(\frac{v - v_0}{\overline{V}} \right)}, & v \geq v_0 \end{array} \right\}. \tag{3}$$

Here $\varphi(v)$ is volume fraction of solute #1 in the outgoing solution and parameter V_i^* represents variation of pulze size. If the peak shape was exactly described by this function then V_i^* would be equal to the injected volume of solute #1.

Optimization of the parameters V_i^*, v_0, $\overline{V}$, and N for each peak was accomplished using a non-linear least-squares procedure. The optimized parameters fit the individual peaks quite well with the exception of a very small secondary tail at the end of the larger peaks which was ignored because its intensity was very small.

After each individual peak was fit, the dependence of V_i^*, v_0, $\overline{V}$, and N on segment number j and injected volume V_i was studied. Parameter V_i^* was found to vary linearly with V_i as expected ($V_i^* = 0.9356\ V_i$, $r^2 = 0.995$, $n = 25$). For experimental convenience, V_i^* was fit with the y-intercept set at 0 to avoid negative values. The volume offset, v_0, varied with segment number ($v_0 = 2.062j - 16.40\ \mu l$, $r^2 = 0.9999$, $n = 25$). However, $\overline{V}$ and N did not behave well at first. Careful examination of the parameters revealed that the covariance between these two parameters in Eq. (*3*) is significant. To account for this problem, the peaks were re-fit holding either $\overline{V}$ or N fixed while the other parameter was optimized. This procedure was repeated until the values converged. In this process, N was found to depend linearly on position ($N = -0.0789j + 8.206$, $r^2 = 0.95$, $n = 25$) while $\overline{V}$ did not ($\overline{V} = 2.748 \pm 0.060\ \mu l$, 1 s, $n = 25$). Neither parameter was found to be dependent on injected volume.

From Theoretical Model to Selectable Gradients

The differences between the fluidic and electronic pulse modulation is such that the theory of the latter can be used as an initial guess to optimize the pulse sizes of the former. To accommodate the difference, the shape of an individual microfluidic peak was fit to a numerical function. Next, the parameters of this function characterized as the peak size and position in the gradient program were changed. At this point, the entire pulse modulation gradient may be simulated by summing numerical functions for each individual peak to create the whole gradient shape. Finally, the size of each pulse was adjusted to optimize the gradient shape so that it matched the desired peak shape. A spreadsheet was developed using Excel (Microsoft, www.microsoft.com) which allows the user to define the desired gradient by adjusting parameters on the following equation:

$$\varphi(v) = a_0 + a_1 v + a_2 v^2 + a_3 v^3 + a_4 \mathrm{e}^{a_5 v} + \frac{a_6}{a_7 + v}, \qquad (4)$$

where a_0–a_7 are user-adjustable coefficients, v is volume in µl, and $\varphi(v)$ is the volume fraction of solute #1. By adjusting the parameters a_0–a_7, linear, quadratic, cubic, exponential, and inverse gradients may be defined. A linear gradient which increases to 0.5 volume fraction of solute #1 is shown in Fig. 5 (· · · ·). The spreadsheet then modulates the gradient shape into 40 pulse sizes. These pulse sizes are used as input by the empirical model, which predicts the gradient shown in Fig. 5 (- - - -). The solver function in Excel may now be used to optimize the pulse sizes. The solver function is constrained to keep each pulse positive and less than the maximum injection size which is the total gradient volume divided by the number of pulses (40). The optimized model shape is shown in Fig. 5 (——). The final performance of the empirical model can be judged by the agreement of its predictions with the experimental gradient, as shown in Fig. 5 (▲). The residuals – the difference between the programmed and experimental gradients – are shown in Fig. 5 (- · - · -). Ideally, the residuals should be randomly distributed, as any significant structure indicates that the pulse program should be improved.
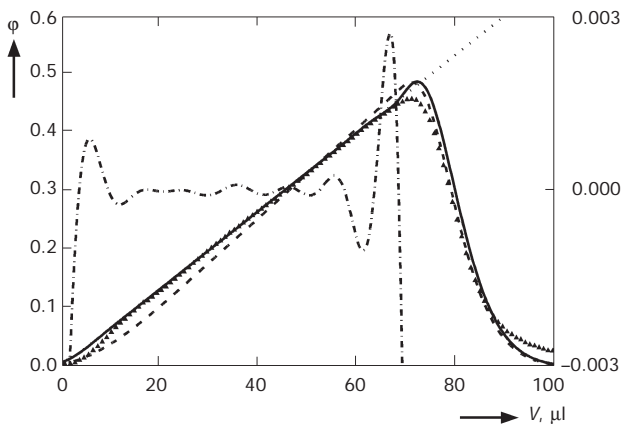

FIG. 5

Performance of the linear gradient: desired linear gradient (· · · ·); predicted PM gradient (- - - -); optimized gradient prediction (——); instrument response (▲); residual between optimized gradient and desired linear gradient (- · - · -). Data plotted as volume fraction of solute #1 (φ) *vs* volume (v) in µl. Residuals (- · - · -) plotted on a 100 times expanded scale. Linear-regression fit in the range from 15 to 65 µl yields a slope of 0.00760 µl^{-1} (r^2 = 0.99996, n = 250) for the PM prediction, 0.00667 µl^{-1} (r^2 = 0.999995, n = 250) for the optimized gradient prediction, and 0.00665 µl^{-1} (r^2 = 0.99993, n = 31) for the instrument response

Resulting Gradients

Experimental gradients with linear, flat, and inverse shapes were generated as shown in Fig. 6. The linear gradients were generated with different slopes rising to 0.25, 0.50, and 0.75 volume fraction of solute #1 (Fig. 6b). Flat gradients were generated with heights of 0.10, 0.25, 0.50, and 1.0 (Fig. 6a). The gradient shown in Fig. 6c was programmed to have a starting value of 0.05 at 5 µl from the start of the gradient and increase along a $1/v$ curvature to 1.0 at 75 µl.

In order to evaluate these gradients, three main factors have been selected: usable range, line-fit parameters and structure of residuals. The usable range is defined as the area of the gradient which is within selected tolerance of the programmed gradient value, such as 1% of the maximum value. The parameters of a least squares fit to a straight line indicate how well the experimental gradient matches the programmed shape. Thus for example, with a linear gradient, the experimental gradient slope should agree with the programmed value. The correlation coefficient, r^2, can also be used to evaluate the gradient. These parameters are summarized in Table II.
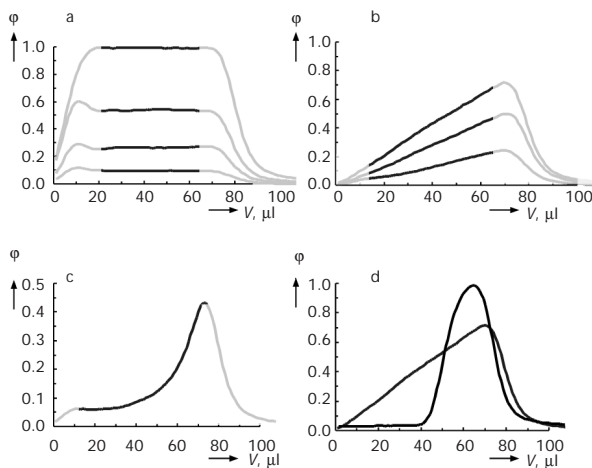

Fɪɢ. 6

Actual FIAgrams achieved from programmed gradients plotted as volume fraction of solute #1 (φ) *vs* volume (*v*) in µl. a Flat gradients with heights of 0.10, 0.25, 0.50, and 1.0. b Linear gradients increasing to 0.25, 0.50, and 0.75. c Increasing inverse gradient. d Comparison of natural FI peak and programmed linear gradient – volume of injected dye is the same, 27.8 µl

Finally, to illustrate the power of pulse-modulation techniques for gradient generation, the "natural" peak shape obtained by a single injection of dye into the gradient coil is compared with a linear gradient obtained with an equal amount (27.8 µl) of the injected dye (Fig. 6d).

CONCLUSIONS

The majority of flow injection methods published to date are based on the readouts such as peak height or peak area while the information contained within the shape of the response peak is not being exploited. The exceptions are so called gradient techniques – FI titrations and stopped-flow reaction rate measurements, which have been so far based either on the "natural" gradients formed in tubular conduit or on the exponentially decreasing peak tail (Fig. 1a) predicted by the single-mixed-tank model[12]. The approach verified in this communication is a novel way to generate desirable gradient shapes within an SI system. This approach is the first step toward development of a system which will perform automated calibrations using a single standard solution, flow-based titration with linear rather than logarithmic response, and kinetic measurement of association and dis-

TABLE II
PM gradient performance. For each type of gradient, performance is quantified by examining statistical parameters of a least-squares line fit

Parameter	Flat (Fig. 6a)				Linear (Fig. 6b)		
	0.10	0.25	0.50	1.0	0.25	0.50	0.75
Range, µl	30–65				15–65		
Theoretical slope, μl^{-1}	0				0.00333	0.00667	0.0100
Slope, μl^{-1}	0.0001	0.0000	0.0001	–0.0002	0.00422	0.00665	0.0105
Theoretical Y-intercept	–[a]				0		
Y-Intercept, µl	–[a]				–0.04146	–0.02295	–0.00023
Height	0.96	0.266	0.540	0.993	–[a]		
r^2 ($n = 31^{[b]}$)	–[a]				0.9997	0.99993	0.99996
s ($n = 31^{[b]}$)[c]	0.001	0.002	0.003	0.002	–[a]		

[a] Not applicable. [b] Number of data points involved in statistical calculation. [c] Sample standard deviation.

sociation rates of antibody/antigen complexes[14,15]. The study of live cell responses to agonists and antagonists[16], would also benefit by application of these programmable concentration gradients.

Single-Standard Calibration

Automated, single-standard calibration will be performed by applying the linearly increasing gradient (Fig. 6b) to the detector, with the slope and range of concentration selected to cover the intended calibration range. For this application, solute #1 will be a standard solution and solute #2 will be the carrier. It is anticipated that process-control applications, where use of multiple serially diluted standards is not practical, will benefit from this approach, in particular, instruments with rapid response times such as UV-VIS, FTIR and Raman spectroscopy. For calibration of electrochemical sensors with slower response times, the flat gradient (Fig. 6a) can be employed. Alternatively, the linear gradient can be delivered in a stepwise fashion, stopping the flow when the gradient has reached a certain concentration. Even so, conditions for assay of individual samples may differ substantially from a readout obtained from a long concentration gradient due to hysteresis of the sensor.

Linearized Flow-Based Titrations

Flow-based titrations will be performed by alternate injections of solute #1 (analyte) and solute #2 (titrant). During the passage of the assembled gradient through the detector, the element of fluid within which the equivalent amounts of titrant and analyte are located marks the end point of the titration. Our initial results show that titration by the inverse gradient generates a linear concentration response producing greater accuracy than the logarithmic calibration used in the traditional flow-injection titration.

Kinetic Measurement of Association and Dissociation

Association and dissociation rates of biomolecules are often studied in two-phase system where ligand is attached to a solid support while the captive biomolecule is in solution passing along the monitored solid support. These studies are carried out by applying a square impulse of the dissolved biomolecule where the concentration is changed suddenly from zero to a steady-state level (for association) and then dropped back to zero (dissociation). The closest to this ideal case are the "flat profiles" (Fig. 6a) obtained

in this work. It is believed that programming of such "flat" gradients will find its use for bioligand interaction studies carried out by BI (ref.[17]). However, a method must be employed to eliminate the non-ideal portion of the "flat" gradients. Recent work by Shank-Retzlaff and Sliger[15] indicates that application of linear or logarithmic gradients combined with numerical analysis may allow one-step measurement of the kinetic constants.

Limitations

Comparison of desirable (Fig. 1) with attainable gradients (Figs 5 and 6) reveals the limitations of the present approach. The grey areas covering the initial and tailing sections of the generated profiles differ significantly from a desired shape. Clearly, gradient programming, however sophisticated cannot entirely eliminate the "natural" tendency of laminar flow through a tubular conduit to promote dispersion between adjacent liquid segments. This is most evident for a "square" profile that has substantial leading and tailing sections. The influence of these sections on the linear gradient to be used for automated calibration is not serious as only the data collected from strictly linear section will be used. The same applies to titrations where the initial distortion of the gradient will affect only the response of most diluted samples. For bioligand interaction studies, the rise and tailing gradient sections are unwelcome and need to be eliminated, most conveniently by stream switching.

REFERENCES

1. Ruzicka J., Hansen E. H.: *Anal. Chim. Acta* **1975**, *78*, 145.
2. Hansen E. H.: *Internet FIA Database*, www.flowinjection.com/search.html.
3. Chalk S.: *Flow Analysis Database*, www.fia.unf.edu.
4. Ruzicka J., Hansen E. H.: *Anal. Chem.* **2000**, *72*, 212A.
5. Scampavia L. D., Hodder P. S., Lähdesmäki I., Ruzicka J.: *Trends Biotechnol.* **1999**, *17*, 443.
6. Ruzicka J.: *Analyst* **2000**, *125*, 1053.
7. Levenspiel O.: *Chemical Reaction Engineering*, 2nd ed. Wiley, New York 1972.
8. Braithwaith A., Smith F. J.: *Chromatographic Methods*, p. 282. Chapman & Hall, London 1996.
9. Wang X. D., Cardwell T. J., Cattrall R. W., Jenkins G. E.: *Anal. Commun.* **1998**, *35*, 97.
10. Magnuson M. L., Kelty C. A.: *Anal. Chem.* **2000**, *72*, 2308.

11. Wang H., Hackett M.: *Anal. Chem.* **1998**, *70*, 205.
12. Cattermole K. W.: *Principles of Pulse Code Modulation*, p. 114. American Elsevier Publishing Company, Inc., New York 1969.
13. Ruzicka J., Hansen E. H.: *Flow Injection Analysis*, 2nd ed. John Wiley & Sons, New York 1988.
14. Karlsson R., Michaelsson A., Mattsson L.: *J. Immunol. Methods* **1991**, *145*, 229.
15. Shank-Retzlaff M., Sliger S. G.: *Anal. Chem.* **2000**, *72*, 4212.
16. Hodder P. S., Beeson C., Ruzicka J.: *Anal. Chem.* **2000**, *72*, 3109.
17. Ruzicka J., Ivaska A.: *Anal. Chem.* **1997**, *69*, 5024.

Jaromir (Jarda) Ruzicka is a professor of Chemistry at the University of Washington (Seattle, U.S.A.), member of the Danish Academy of Technical Sciences and past president of the Danish Society for Analytical Chemistry. He was born in Prague in 1934, where he also graduated from Charles University, Department of Analytical Chemistry and where he worked as assistant to prof. F. Běhounek at Department of Nuclear Chemistry at the Faculty of Nuclear Physics, together with A. Zeman and J. Starý.

In 1968 he emigrated to Denmark, where he obtained a position at the Technical University of Denmark. There, he became, ten years later, a full professor, holding a chair that was then, for the first time in Denmark, awarded to the field of analytical chemistry. During this time, in 1974, he co-invented with his colleague E. H. Hansen, the flow injection method. FI found its first practical applications in Brazil, where J. R. served in 1975 as an expert for United Nations Development Agency. In Seattle, at Department of Chemistry and in the Center for Process Analytical Chemistry, his research has been since 1987, aimed at further development of flow injection, resulting in concepts of sequential injection, bead injection and microfluidic based automated assays, applied to drug discovery, immunoassays and bioassays. J. R. published two monographs, close to 300 papers and was granted over a dozen of patents in the U.S.A. and E.U. Amongst his scientific awards are Talanta Medal, the Torben Bergman Medal by the Swedish Chemical Society, the Gairn Medal by the Scientific Council of European Community, The Memorial Medal by Charles University and The Silver Medal by the University of Warsaw.

He has four children and six grandchildren living in Seattle, and in Copenhagen. His hobbies are snowboarding and skiing in winter, and coastal navigation when weather is clement on the West Coast.